



Missouri University of Science and Technology
Scholars' Mine

International Specialty Conference on Cold-Formed Steel Structures

(1986) - 8th International Specialty Conference on Cold-Formed Steel Structures

Nov 11th, 12:00 AM

Cold-formed Steel Compression Members Embedded in Grain

Ahmed Sabry

George Abdel-Sayed

Follow this and additional works at: <https://scholarsmine.mst.edu/isccss>

 Part of the [Structural Engineering Commons](#)

Recommended Citation

Sabry, Ahmed and Abdel-Sayed, George, "Cold-formed Steel Compression Members Embedded in Grain" (1986). *International Specialty Conference on Cold-Formed Steel Structures*. 2.
<https://scholarsmine.mst.edu/isccss/8iccfss/8iccfss-session6/2>

This Article - Conference proceedings is brought to you for free and open access by Scholars' Mine. It has been accepted for inclusion in International Specialty Conference on Cold-Formed Steel Structures by an authorized administrator of Scholars' Mine. This work is protected by U. S. Copyright Law. Unauthorized use including reproduction for redistribution requires the permission of the copyright holder. For more information, please contact scholarsmine@mst.edu.

COLD-FORMED STEEL COMPRESSION MEMBERS EMBEDDED IN GRAIN

By

Ahmed Sabry⁽¹⁾ and George Abdel-Sayed⁽²⁾

SUMMARY

The present paper deals with thin walled axially loaded members embedded in granular material. It examines the restraining effect of the granular mass on the displacement and post-buckling behaviour of components such as vertical stiffeners used in flexible grain bins.

The analysis and the experimental program show an increase of at least 50% in the load carrying capacity of a stiffener embedded in grain.

INTRODUCTION

Grain bins made of cold-formed steel are widely used for the on-farm grain storage, Fig. 1a. Their design is governed mainly by the horizontal and vertical components of grain pressure induced on the walls. The walls are often built of horizontally corrugated panels of very low vertical rigidity while vertical stiffeners are provided to carry the vertical load. These stiffeners are built of cold-formed steel members of sections such as angles, channels or z-sections.

The vertical load carrying capacity of the bin walls is governed by two limit states:

(1) Research Assistant, Dept. of Civil Eng., Univ. of Windsor, Windsor, Ontario, Canada.

(2) Professor, Dept. of Civil Eng., Univ. of Windsor, Windsor, Ontario, Canada.

1) The overall buckling of the stiffened cylindrical wall of the bin which has been examined by Ghobrial and Abdel-Sayed (1). Herein, the stiffened bin walls are treated as if being made of equivalent orthotropic material. This analysis does not account for any failure of the individual stiffeners.

2) The vertical stiffeners are bolted to the corrugated panels in a skips distribution as shown in Fig. 1b. Therefore, their load carrying capacity could be governed by the capacity of the axially loaded, unsupported zone of the stiffeners.

At the present time, the ultimate load carrying capacity of the axially loaded vertical stiffeners is determined with no consideration to their being embedded in grain. However, the load carrying capacity is in fact affected by the interaction between the lateral displacements of the plate components of the stiffeners and the pressure of the granular material.

The objective of the present paper is to examine the restraining effect of the granular mass on the displacements of the stiffeners and their corresponding post-buckling behaviour. The study is based on a nonlinear elastic-plastic finite element computer program developed by Sabry (5). This program analyses the large-order displacement of the stiffener and its plate components embedded in grain. An experimental program was undertaken in the course of the present study showing good agreement between theoretical and experimental results.

ANALYSIS

An incremental finite element analysis is employed to deal with the problem of large-order displacements and material nonlinearity in axially

loaded thin walled members. The effect of the grain surrounding the stiffeners is accounted for as lateral elastic supports (5).

The total potential energy is evaluated as a function of the nodal displacement components. Differentiating the total potential energy leads to a non-linear set of equations which governs the behaviour of the stiffener. The solution is obtained through iterative approach using the Newton-Raphson process and the following incremental matrix equation (5, 6):

$$[K_e + K_{eL} + K_G + k]\{d\} = \{P\} \quad (1)$$

where $[K_e]$ is the linear elastic stiffness matrix

$[K_{eL}]$ is the initial displacement stiffness matrix

$[K_G]$ is the initial stress stiffness matrix

$[k]$ is the stiffness matrix accounts for the spring effect of the granular material

$\{d\}$ is the incremental displacement vector

$\{P\}$ is the incremental load vector

Von Mises criterion is used in the present study for the yield limitation. The relation between the stresses and strains in the inelastic stage is a function of the stresses based on Prandtl-Ruses flow theory (2). The analysis is given in detail by Sabry in reference (5).

The behaviour of stiffeners in grain bins and the effect of their being embedded in the granular mass is illustrated through the analysis of stiffeners of two different cross-sections. The first example deals with an angle 2.0 x 2.0 in (50.8 x 50.8 mm) and 30 in. (762 mm) of unsupported height, Fig. 1b. In that example, two different thicknesses are considered, 0.06 in (1.524 mm) and 0.075 in (1.9 mm) for sections "A1" and "A2", respectively. The second example, B, is a channel cross-section 8.0

x 2.0 in (203.2 x 50.8 mm) with unsupported height of 30 in (762 mm) and thickness of 0.06 in (1.524 mm).

The effect of the granular material is presented as lateral elastic supports along the stiffeners. Herein, the modulus of grain reaction is a function of the modulus of elasticity for the granular material. For comparison, a case of no granular material around the stiffener (i.e. $E_g = 0$) is examined together with cases of modulus of elasticity for the granular material equal to 500, 1000, 2000 and 3000 psi (3.5, 7.0, 14.0 and 21.0 MPa). The above range of E_g is chosen to cover the actual range for the modulus of elasticity which falls between 1500-2000 psi (10.5-16.25 MPa) as suggested by Manbeck (3).

ANGLE STIFFENERS

a) Relation Between Load and Lateral Displacement

Figs. 2 and 3 show the non-linear relation between the axial force and the magnitude of the lateral displacement of the unsupported leg at mid-height of sections A1 and A2, respectively. This load-displacement relation can be considered in evaluating an equivalent buckling load at the intersection of the initial tangent and the tangent at the point of inflection as suggested by Kinloch (2). The thin angle, A1, reaches its failure conditions within the elastic limit for all cases while the load carrying capacity of the thick angle A2 is governed by the yield limit, especially when embedded in granular material. In that example the yield stresses are considered equal to 42000 psi (288 MPa).

The relation between the modulus of the surrounding material and the equivalent buckling load of angle A1 is plotted in Fig. 4 including the case of no surrounding granular material ($E_g = 0$). The stiffener embedded

in granular material with $E_g = 500$ psi (3.5 MPa) has a load carrying capacity of 1.5 times that of the stiffener without surrounding granular material. However, further increase in the modulus of the granular material does not have proportional effect on the load carrying capacity of the angle.

The deformed shape of angle A1, at the equivalent buckling load, is shown in Fig. 5a for the case with no surrounding grain and in Fig. 5b when being embedded in grain with $E_g = 500$ psi (3.5 MPa). Herein, it is noted that the position of the maximum deformation in the unsupported leg of the angle changes from the mid-height in angle with no grain to near the ends when embedded in grain. Also the number of buckling waves increases from seven when $E_g = 0$ to eleven when $E_g = 500$ psi (3.5 MPa).

b) Stress Distribution

At the early increments of loading, the stresses are uniform over the cross-sections. As the load approaches the level of local buckling, stress concentration starts to develop near the bend between the two plate elements. Fig. 6a and 6b show the stress distributions over the section of the angle A1 at the equivalent buckling load for the case without and with surrounding grain, respectively.

CHANNEL STIFFENER

The relationship between the load and the lateral displacement at mid-height of the web is presented in Fig. 7. From this figure the equivalent buckling load is evaluated and presented in Fig. 4 versus the modulus of the granular material. Herein, it is noticed that the same as for the angle sections, the rate of increase of the equivalent buckling load is reduced with the increase of the modulus E_g .

Fig. 8a shows the buckling waves of the free channel to have five waves, while this number is increased to eleven waves, Fig. 8c, when the surrounding grain has $E_g = 2000$ psi (14.0 MPa).

Fig. 9a and 9b show the stress distribution over the channel cross-sections. These stresses are uniformly distributed at the initial load increments and become concentrated at the corners as the web deflects laterally when the load approaches or reaches the equivalent buckling load.

TEST RESULTS

In the course of the present study, the angle A1 is tested under axial loading (5) with and without being embedded in granular sand. The test results of both lateral displacement at the edge of the unsupported leg and the maximum stresses at the corner of the angle are compared in Figs. 10 and 11. Herein, the case for the stiffener with no surrounding sand is compared with tests a and b, Fig. 10. However, for the stiffener embedded in sand, the ultimate load carrying capacity is recorded experimentally to be 6000 psi (42.0 MPa) and is reported in Fig. 10 together with the corresponding analytical results. Herein, Fig. 10 and 11 show the test results agree with the analysis is the main trend of behaviour of the stiffeners. Yet some differences remain in the magnitude of deflection or stress concentration. These are attributed to the presence of some irregularity of the corrugated sheet which caused either the top or bottom connection with the stiffener to be slightly loose, i.e. allowing for some eccentricity. Therefore, the theoretical point of start of stress concentration is higher than the corresponding experimental value by about 10% - 20% in both cases of empty and filled bin Fig. 10 and 11.

CONCLUSION

The study for the behaviour of the bin's longitudinal stiffeners embedded in the granular material leads to the following:

1. The load carrying capacity of the bin's vertical stiffeners is increased by at least 50% as a result of accounting for the grain surrounding them.

2. The higher values of the modulus of elasticity for the grain has little effect on the load carrying capacity of the stiffener. This allows the engineer to assume any reasonable value for the grain modulus with no significant effect on the results.

3. The number of the local buckling waves are increased as a result of the granular material effect. This takes place with reduced magnitude of displacement because of the restraining effect of the grain.

4. The axial stresses are concentrated near the bend between the two plate elements when the incremental load approaches the buckling limit. Failure is usually triggered when the concentrated stresses reach the yield limit.

APPENDIX I: REFERENCES

1. Ghobrial, M. and Abdel-Sayed, G., "Stability of Orthotropic Cantilever Cylindrical Shells"; Proc. of the International Conference on Thin-Walled Structures, University of Strathclyde, Scotland, Granada Publishers, 1980, pp. 351-370.

2. Kinloch, H. and Harvey, J.M., "Analysis and Design of Anisotropic Plate Structure with Particular Reference to Decking System," edited by A.H. Chilver, Thin Walled Structures, John Wiley & Sons, Inc., New York, 1967, pp. 271-299.
3. Little, G.H., "Rapid Analysis of Plate Collapse by Live Energy Minimization", Int. J. Mech. Sci., Vol. 19, Pergamon Press 1977, Printed in Great Britain, pp. 725-744.
4. Manbeck, H.B., "An Experimental Study of the Three Dimensional Stress-Strain Behaviour of Wheat En Masses", Unpublished Ph.D. Thesis, Oklahoma State University, Stillwater, Oklahoma, 1970.
5. Sabry, A., "Thin Walled Stiffeners in Flexible Grain Bins", Ph.D. Thesis presented to University of Windsor, Civil Engineering Dept., 1986.
6. Zinkiewicz, O.C., The Finite Element Method, McGraw-Hill Book Co., New York, 1977.

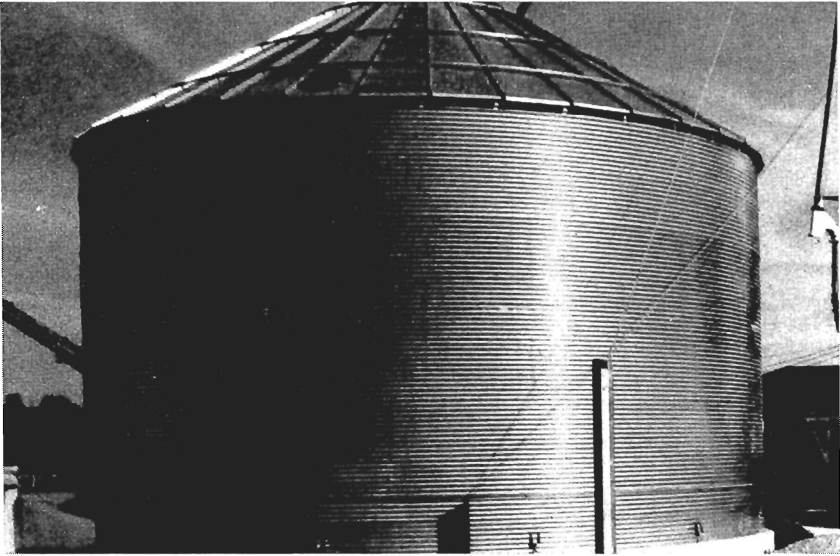


Fig. 1a Grain Bin Structure

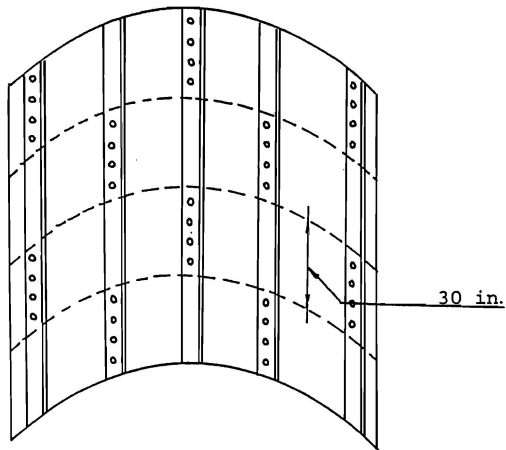


Fig. 1b Arrangement of Bin's Stiffeners

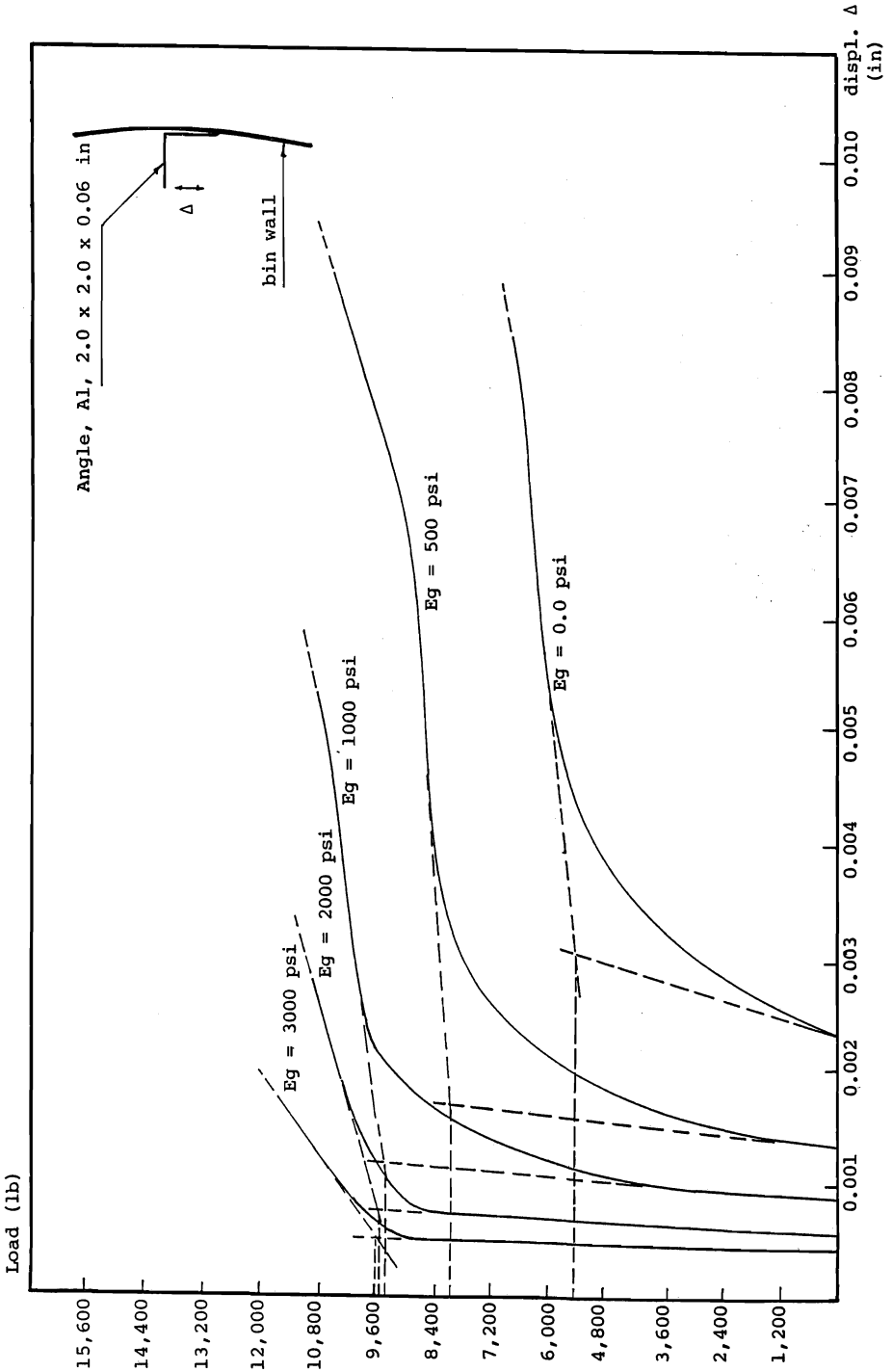


Fig. 2 Load vs. Maximum Horizontal Displacement of Unsupported Leg (1 in. = 25.4 mm)

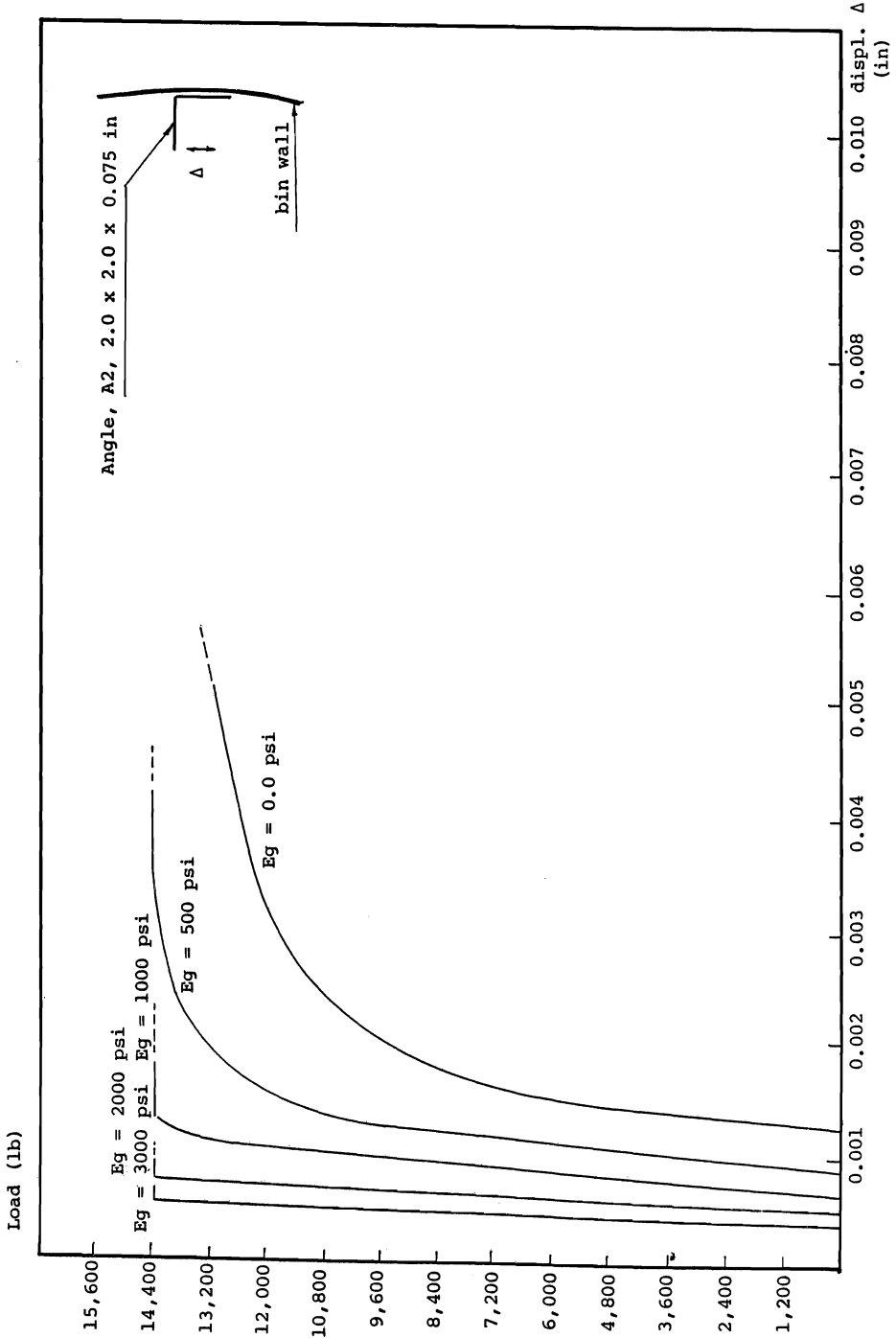


Fig. 3 Load vs. Maximum Horizontal Displacement of Unsupported Leg (1 in = 25.4 mm)

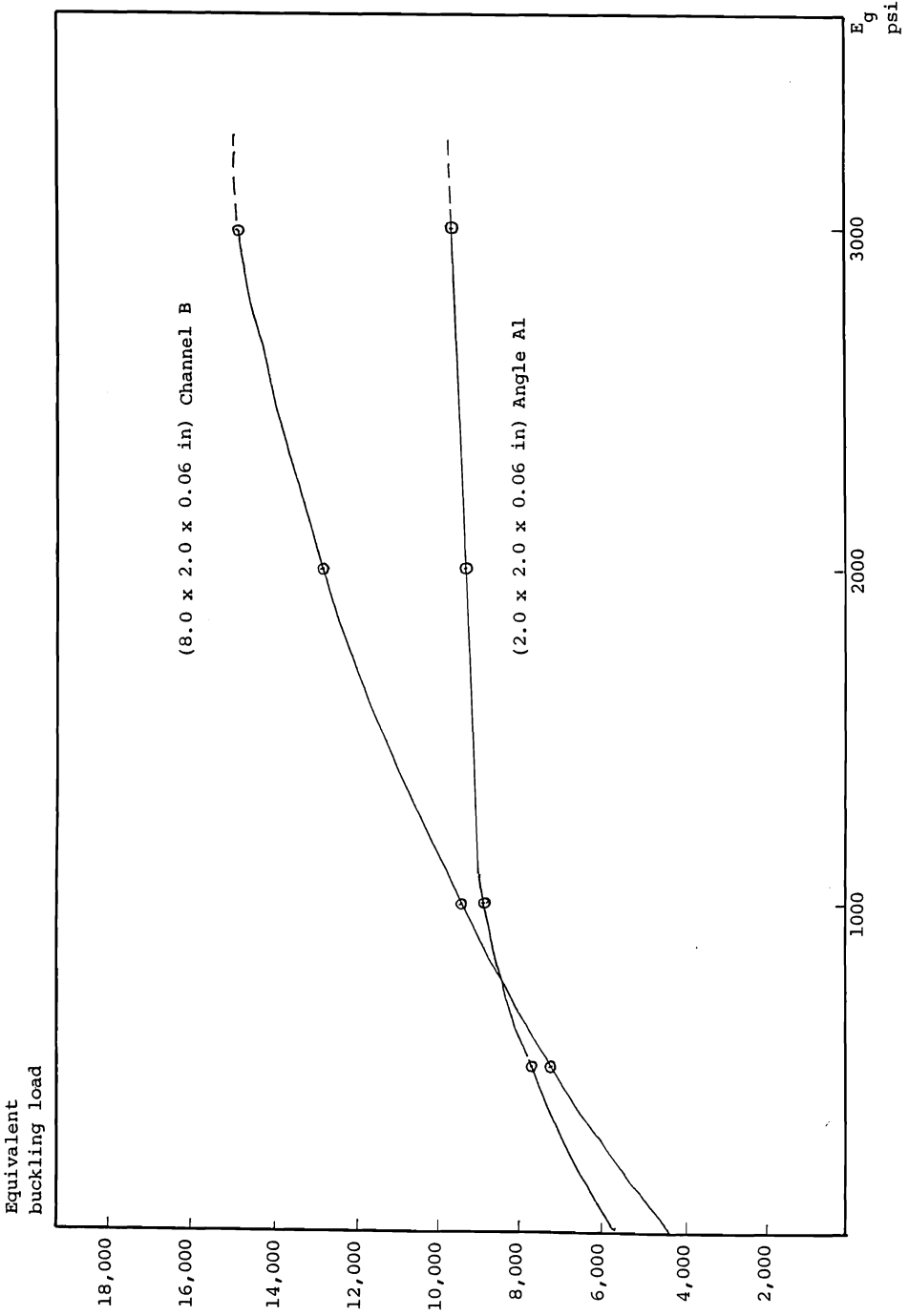


Fig. 4 The Relation Between the Modulus of the Granular Material E_g and the Corresponding Equivalent Buckling Load

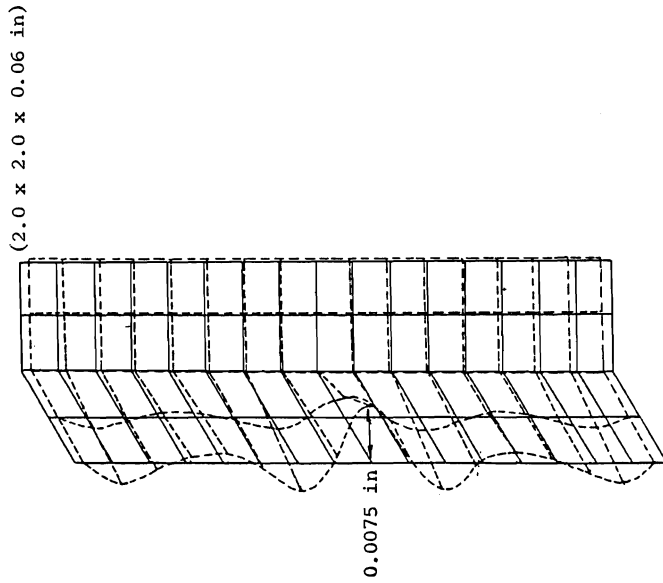


Fig. 5a Deformed Shape of the Stiffener with no Surrounding Granular Material at the Equivalent Buckling Load (6.6 kips)

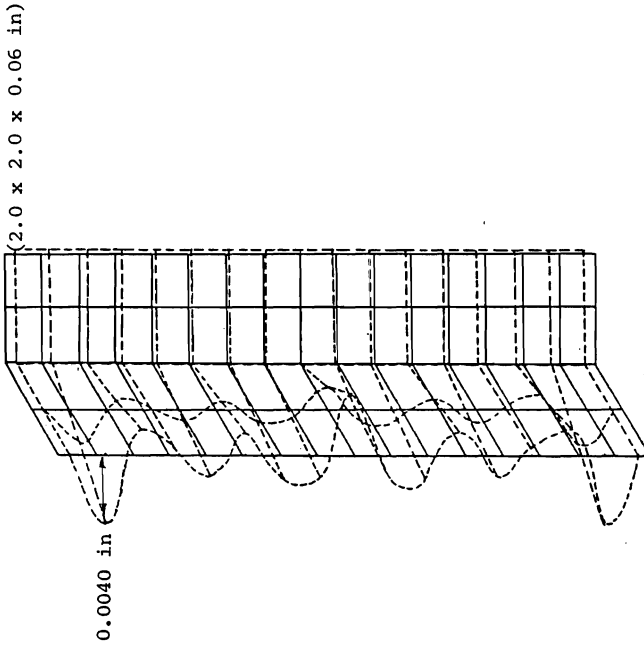


Fig. 5b Deformed Shape of the Embedded Stiffener in the Granular Material with $E_g = 500$ psi at the Equivalent Buckling Load (8.4 kips)

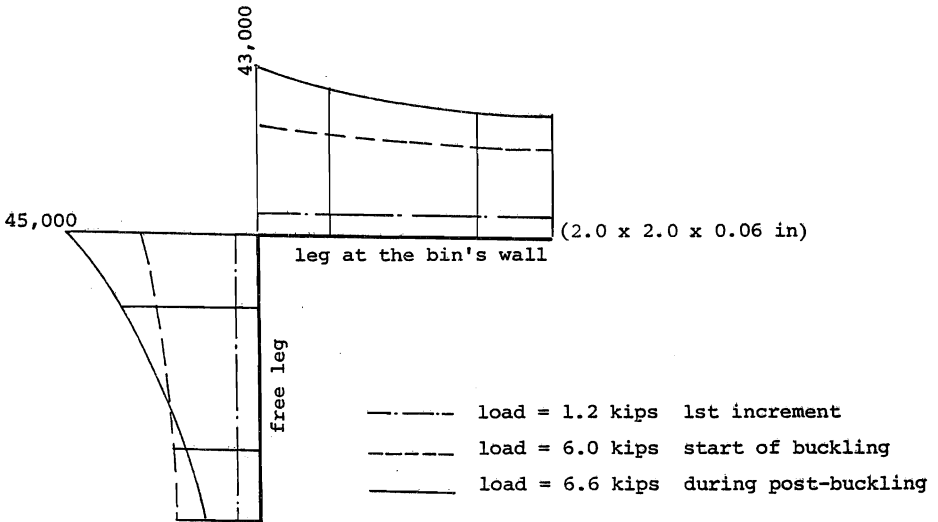


Fig. 6a Stresses Distribution Along the Middle Section in Case of No Surrounding Granular Material
Scale: 1 cm = 16000 psi

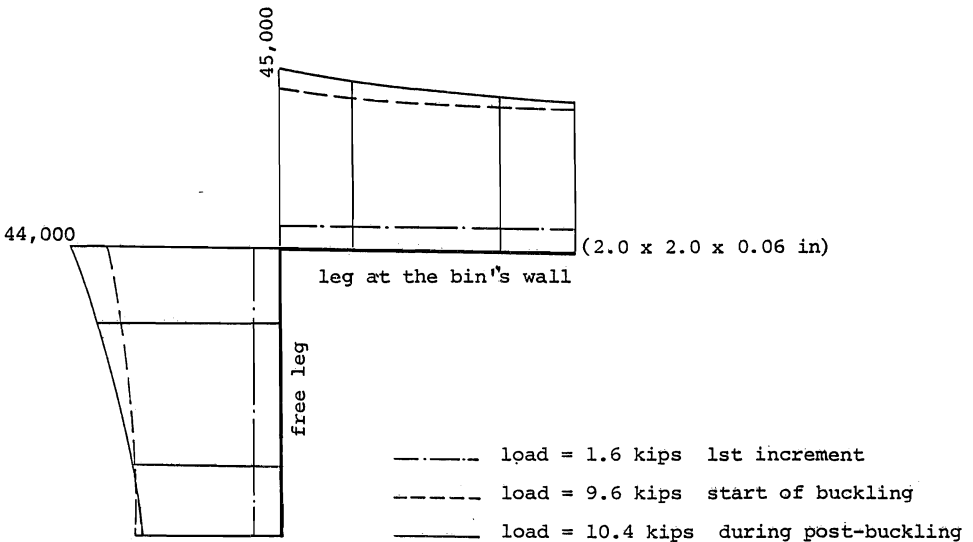


Fig. 6b Stresses Distribution Along the Middle Section in Case of Embedded Stiffener in the Granular Material with $E_g = 2000$ psi
Scale: 1 cm = 16000 psi

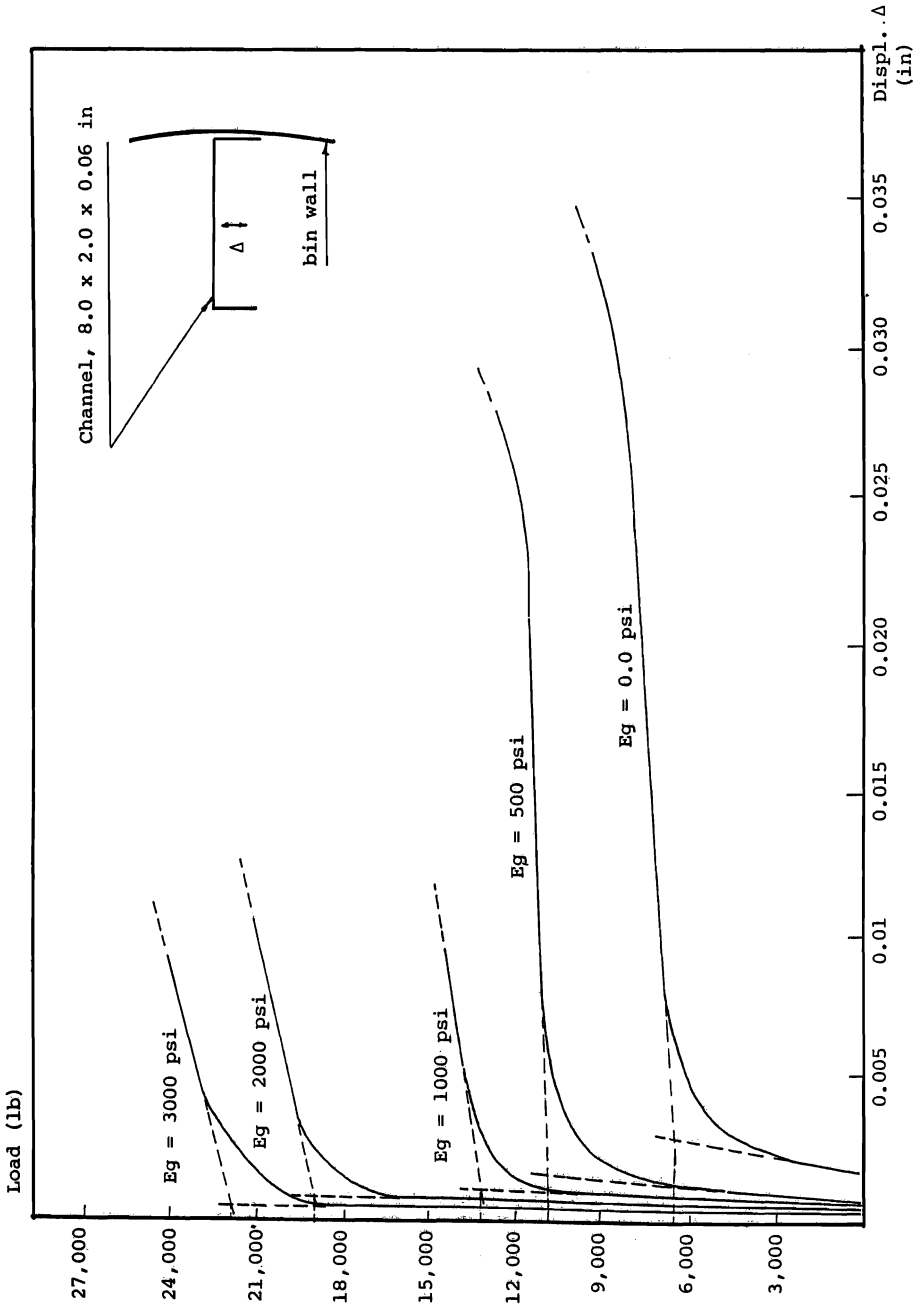


Fig. 7 Load-displacement Curve for Different Values for the Granular Material's Modulus of Elasticity

(8.0 x 2.0 x 0.06 in)

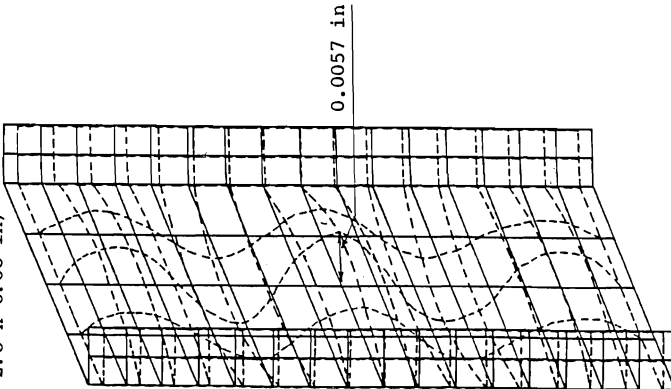


Fig. 8a Deformed Shape of the Free Stiffener at the Equivalent Buckling Load (7.2 kips)

(8.0 x 2.0 x 0.06 in)

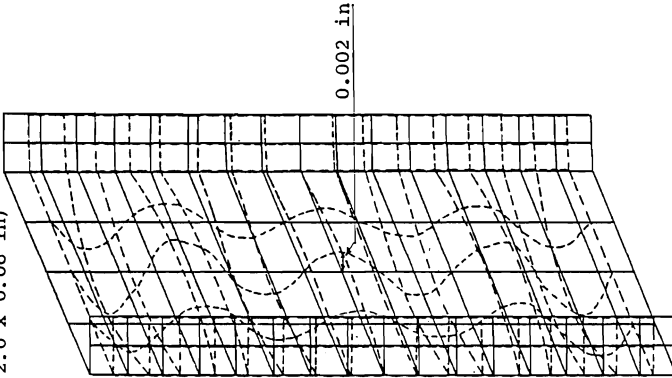


Fig. 8b Deformed Shape of the Stiffener Embedded in the Granular Material with $E_g = 500$ psi at the Equivalent Buckling Load (10.8 kips)

(8.0 x 2.0 x 0.06 in)

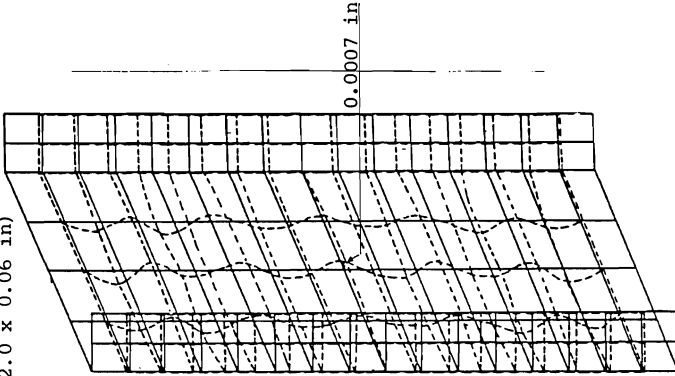


Fig. 8c Deformed Shape of the Stiffener Embedded in the Granular Material with $E_g = 2000$ psi at the Equivalent Buckling Load (18.0 kips)

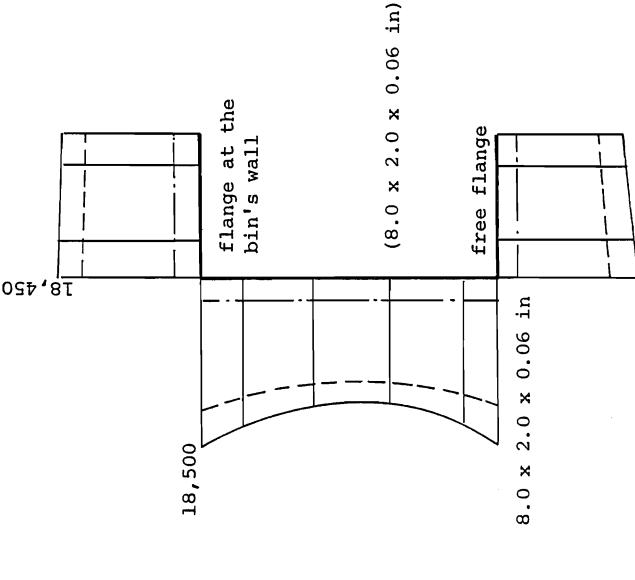


Fig. 9b Stresses Distribution Along the Middle Section in Case of Embedded Stiffener in the Granular Material with $E_g = 500$ psi

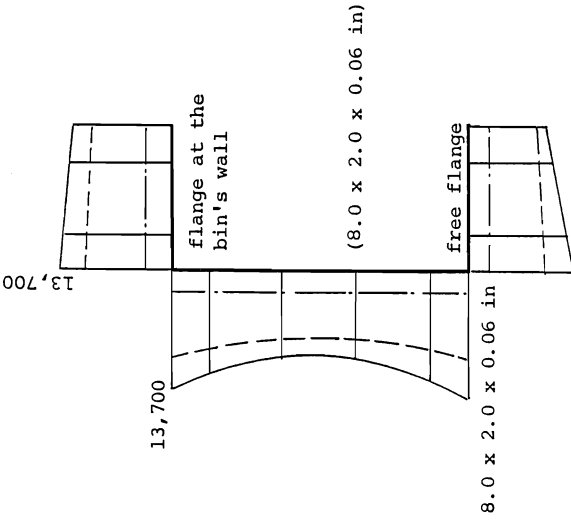


Fig. 9a Stresses Distribution Along the Middle Section in Case of No Surrounding Granular Material

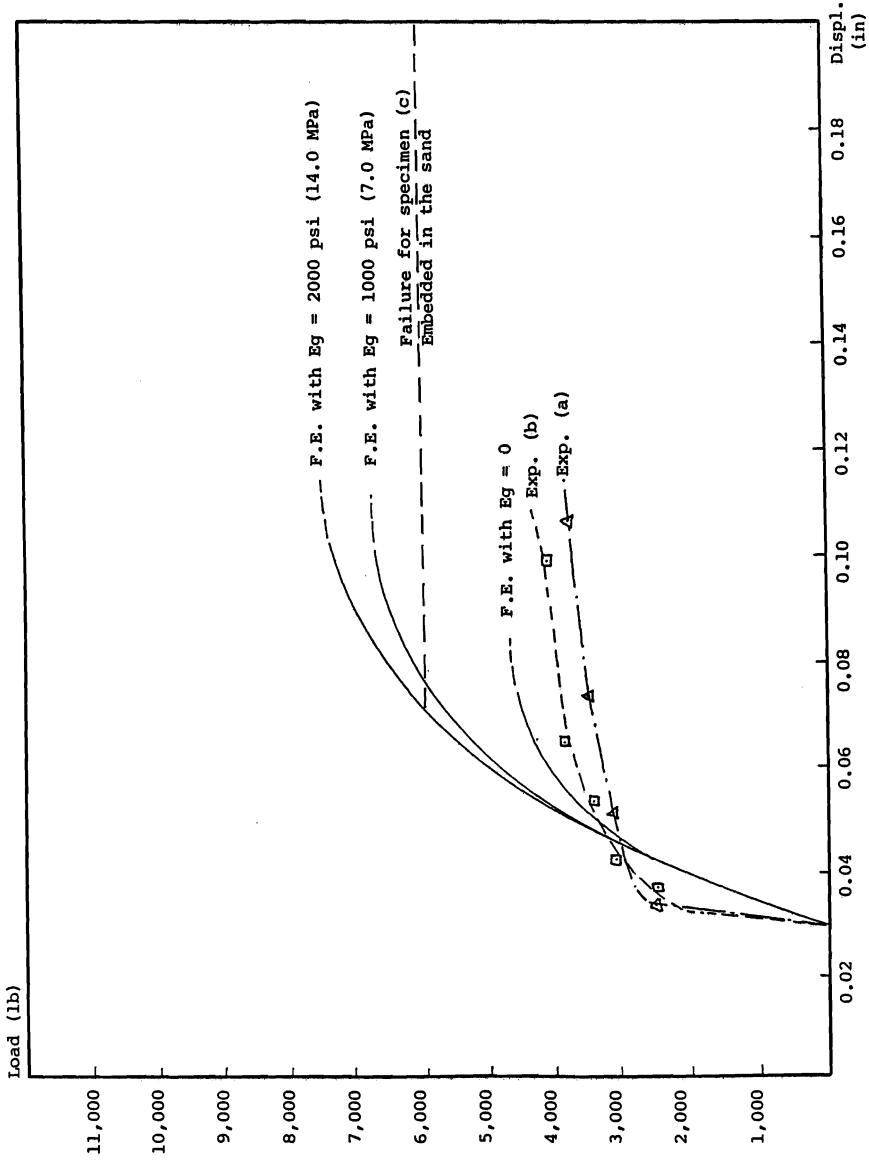


Fig. 10 Experimental and Analytical Relation Between Load and Lateral Displacement

